

# Novel Hollow-Fiber Anion-Exchange Hybrid Membranes: Preparation and Characterization

Tongwen Xu, Fangfang Lu, Yonghui Wu

Laboratory of Functional Membranes, Department of Chemistry, University of Science and Technology of China, Hefei, Anhui 230026, People's Republic of China

Received 6 May 2008; accepted 18 September 2008

DOI 10.1002/app.29368

Published online 11 December 2008 in Wiley InterScience (www.interscience.wiley.com).

**ABSTRACT:** To develop ion-exchange membranes for application in severe conditions, such as those with high temperatures, strongly oxidizing environments, or organic solvents, new hollow-fiber anion-exchange hybrid membranes were prepared by the immersion of brominated poly(2,6-dimethyl-1,4-phenylene oxide) base hollow fibers in a tetraethoxysilane-ethanol solution followed by sol-gel and quaternary amination. Compared to conventional polymeric charged membranes, the prepared hybrid membranes were higher in both thermal and dimensional stabilities. The results suggest that tetraethoxysilane concentration was an important

factor affecting the membrane's intrinsic properties. When the tetraethoxysilane concentration was in the range 15–45%, the final hollow-fiber anion-exchange hybrid membranes had an ion-exchange capacity of 1.9–2.0 mmol/g, a water uptake of 83–1.23 g of water/g of dry weight, and a dimensional change ratio of 13–18%. An evaluation on the membranes' separation performances is underway. © 2008 Wiley Periodicals, Inc. *J Appl Polym Sci* 111: 3128–3136, 2009

**Key words:** separation techniques; poly(phenylene oxide); ion exchange membrane

## INTRODUCTION

An ion-exchange membrane is generally defined as an ion-exchange resin in membrane shape. This definition leads to a classification analogous to that of ion-exchange resins. For example, traditional ion-exchange membranes are classified as anion-exchange and cation-exchange membranes according to the type of ionic groups attached to the membrane matrix. Cation-exchange membranes contain negatively charged groups, such as  $-\text{SO}_3^-$ ,  $-\text{COO}^-$ ,  $-\text{PO}_3^{2-}$ ,  $-\text{PO}_3\text{H}^-$ , and  $-\text{C}_6\text{H}_4\text{O}^-$ , which are fixed to the membrane backbone and allow the passage of cations but reject anions. On the contrary, anion-exchange membranes contain positively charged groups, such as  $-\text{NH}_3^+$ ,  $-\text{NRH}_2^+$ ,  $-\text{NR}_2\text{H}^+$ ,  $-\text{NR}_3^+$ ,  $-\text{PR}_3^+$ , and  $-\text{SR}_2^+$ , which are fixed to the membrane backbone and allow the passage of anions but reject cations.<sup>1,2</sup> Unique in ionic selectivity, anion-exchange and cation-exchange membranes can be used together under an electric gradient (termed *electrodialysis*) or alone under a concentration gradient (termed *diffusion dialysis*) in many fields, such as the desalination of sea

water and brackish water, treatment of industrial effluents, concentration or separation of food and pharmaceutical products containing ionic species, and recovery of acids or bases from waste effluents.<sup>2–6</sup> The technology based on ion-exchange membranes can not only make the process cleaner and more energy-efficient but also recover resources from waste discharges and thus make development in society sustainable.

In most cases, ion-exchange membranes have to be applied under severe conditions, such as those with high temperatures, a strongly oxidizing environment, or organic solvents; however, the available organic ion-exchange membranes cannot function well under these conditions. Recently, organic-inorganic hybrid materials have attracted great attention because they can add the advantages of inorganic materials to those of organic materials.<sup>7–11</sup> As for their preparation, three methods can be used: (1) charged precursors (including organically modified alkoxysilanes or alkoxysilane functionalized polymers/oligomers) are used for sol-gel processes, (2) organically modified alkoxysilanes or alkoxysilane-functionalized polymers/oligomers are used for sol-gel processes and subsequent quaternary amination or sulfonation (note that the precursor must contain a moiety that can be transformed into ionic groups in the subsequent chemical reaction), and (3) a single precursor or a mixture of precursors are used for sol-gel processes in the presence of charged organic polymers.<sup>12</sup> With these methods, some anion- and cation-exchange hybrid membranes were prepared in our laboratory. For example, cation-exchange

Correspondence to: T. Xu (twxu@ustc.edu.cn).

Contract grant sponsor: National Science Foundation of China; contract grant numbers: 20774090, 20636050.

Contract grant sponsor: National Basic Research Program of China; contract grant number: 2009CB623403.

hybrid membranes were prepared through sol-gel processes with negatively charged alkoxy-silane-functionalized poly(ethylene oxide) as the sol-gel precursor.<sup>13</sup> Also, we prepared a series of anion-exchange hybrid membranes or materials from positively charged poly(methyl acrylate)-SiO<sub>2</sub> nanocomposites;<sup>14</sup> end-capped poly(ethylene oxide) 400 with the silane containing secondary amine and trialkoxy-silane groups;<sup>15</sup> positively charged brominated poly(2,6-dimethyl-1,4-phenylene oxide) (BPPO) and aminopropyl-trimethoxysilane; and trimethylamine (TMA).<sup>16</sup> According to a search with Web of Science (<http://portal.isiknowledge.com>), the hybrid membranes reported were all flat-plate membranes; however, in some cases, especially in acid or/and base recovery with diffusion dialysis, hollow-fiber modules constructed from hollow-fiber ionic membranes have more advantages, such as maximum mass transfer area per unit volume of the module, the lowest cost, and the lowest weight because of the elimination of clamping plates, spacers, and gaskets.<sup>17</sup> In our previous study, we developed hollow-fiber anion-exchange membranes for this purpose by spinning a BPPO-1-methyl-2-pyrrolidone (NMP) solution and then aminating the fibers.<sup>17</sup> However, the prepared hollow-fiber anion-exchange membranes did not have desirable thermal and dimensional stabilities. Therefore, in this study, we focused on preparing novel hollow-fiber anion-exchange hybrid membranes by treating BPPO base fibers with tetraethoxysilane (TEOS) and then performing sol-gel and quaternary amination. The characterizations and properties of the obtained hollow-hybrid membranes, such as the thermal stability, ion-exchange capacity (IEC), water uptake, and dimensional stability, are fully discussed.

## EXPERIMENTAL

### Materials

The BPPO polymers were kindly supplied by Tianwei Membrane Corp., Ltd. (Shandong, China). In this research, two kinds of BPPOs were used. Theoretically, they had 90% benzyl substitution and 10% aryl substitution (D9010) and 90% benzyl substitution and 20% aryl substitution (D9020), respectively. TMA was a saturated aqueous solution. Other chemicals, such as ethanol, NMP, and TEOS, were analytical grade, and all of them were purchased from a domestic chemical-reagent company. Deionized water was used throughout.

### Preparation of the base hollow fibers

Base hollow fibers were prepared in an industrial spinning line that contained dissolution, filtration, spinning, coagulation, and take-up units. The line

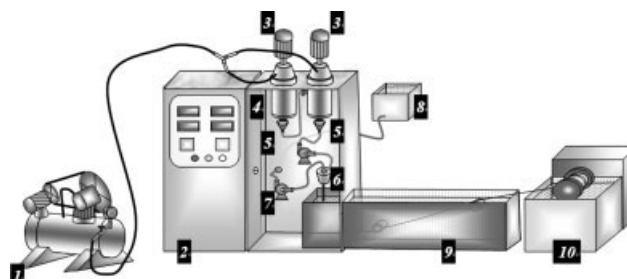


**Figure 1** Schematic of the base hollow-fiber spinning system: (1) air compressor, (2) controllable tank, (3) stirrers, (4) dissolution kettle (left) and filtration kettle (right), (5) 15- $\mu$ m filter, (6) spinneret, (7) syringe pumps (left for bore fluid and right for the polymer solution), (8) bore fluid tank, (9) coagulation bath, and (10) take-up unit and collection bath. Reprinted with permission from ref. 17. Copyright 2008 American Chemical Society.

was schematically shown in our previous article<sup>17</sup> and is reproduced here (Fig. 1). We prepared the dope by dissolving a mixture of BPPO 9010 and BPPO 9020 (0.42 : 0.38 w/w) in NMP (polymer concentration  $\approx$  34.3 wt %); this was then fed into the tanks by an air compressor and filtered by a 15- $\mu$ m filter (metallic net). After it was degassed in the tank for more than 24 h, the dope was driven by high pressure through a 1.5-mm spinneret. Tap water was used as the bore fluid, and its flow rate was controlled by a syringe pump. The spinning process was conducted at room temperature (28–30°C). The liquid fiber dropped under gravity into the coagulation bath (tap water). The liquid fiber was solidified simultaneously by the external coagulation bath and internal bore fluid, which formed the internal and external surfaces, respectively. The solidified fibers were collected with a take-up reel. The hollow fibers were then stored in water for 3 days, with the water replaced every 0.5 days, and dried in air for subsequent treatment. Notably, during phase inversion, the pore structure of the hollow fiber was affected by the composition of the dope and the coagulation bath, temperature, and humidity. This was discussed in our previous article,<sup>17</sup> and the optimum conditions (Table I) were adopted for this research. In this sense, the base hollow fibers prepared had the same microstructure as before.

### Preparation of the hollow-fiber anion-exchange hybrid membranes

The hollow-fiber hybrid membranes were prepared through a sol-gel process with TEOS and subsequent quaternary amination with TMA. Initially, the BPPO hollow fiber with an initial length of  $L_1$  (75 mm) and an initial weight of  $W_1$  was immersed in a TEOS-C<sub>2</sub>H<sub>5</sub>OH solution at room temperature. The volumetric ratios of TEOS to ethanol were set at 0, 5,

TABLE I  
Preparation of the BPPO Base Hollow Fibers

Dope solution	34.3 wt % BPPO mixture in NMP with a BPPO9010/BPPO9020 weight ratio of 1.1 : 1
Bore fluid	Tap water
External coagulant	Tap water
Distance from the spinneret to the coagulation bath (mm)	500
Spinning temperature (°C)	28–30
Size of the spinneret (mm)	1.5
Bore fluid flow rate (mL/min)	0.2–0.3
Frequency controlling the dope flow rate (Hz)	25.8
Frequency controlling the take-up unit (Hz)	12.4
Solvent exchange	3 days in tap water with water replaced every half-day
Drying	Ambient temperature

10, 15, 25, 35, and 45% and so on. The product in this step was denoted as BPPO–TEOS. After 12 h, 0.01 mol/L HCl was added, and its volume was controlled to ensure that the molar ratio of Si/H<sub>2</sub>O was 1 : 6. After 3 h, the fibers, denoted as BPPO–SiO<sub>2</sub>, were taken out, washed, and dried at 70°C for 2 h and then at 90°C for a further 2 h. The length (*L*<sub>2</sub>) and weight (*W*<sub>2</sub>) were determined. Then, these hollow fibers were quaternary aminated with a 1.0M TMA aqueous solution for 24 h at room temperature. Then, the aminated hollow fibers, denoted as BPPO–SiO<sub>2</sub>(+), were washed with deionized water repeatedly to remove the residual alkali. The lengths and weights of the wet fibers in this step were recorded as *L*<sub>3</sub> and *W*<sub>3</sub>, and the corresponding dry

weights were recorded as *W*<sub>4</sub>. The reactions are schematically shown in Figure 2.

### Instrumentation

Fourier transform infrared (FTIR) spectra were recorded with an FTIR spectrometer (Vector 22, Bruker, Ettlingen, Germany) at a resolution of 2 cm<sup>-1</sup> and a spectral range of 4000–400 cm<sup>-1</sup>. In the test, we used the BPPO in the form of a membrane by casting its chloroform solution, whereas the other samples [BPPO–TEOS, BPPO–SiO<sub>2</sub>, and BPPO–SiO<sub>2</sub>(+)] were powdered and mixed with KBr. The thermal behavior was analyzed with a Shimadzu TGA-50H analyzer (Kyoto, Japan) under a nitrogen

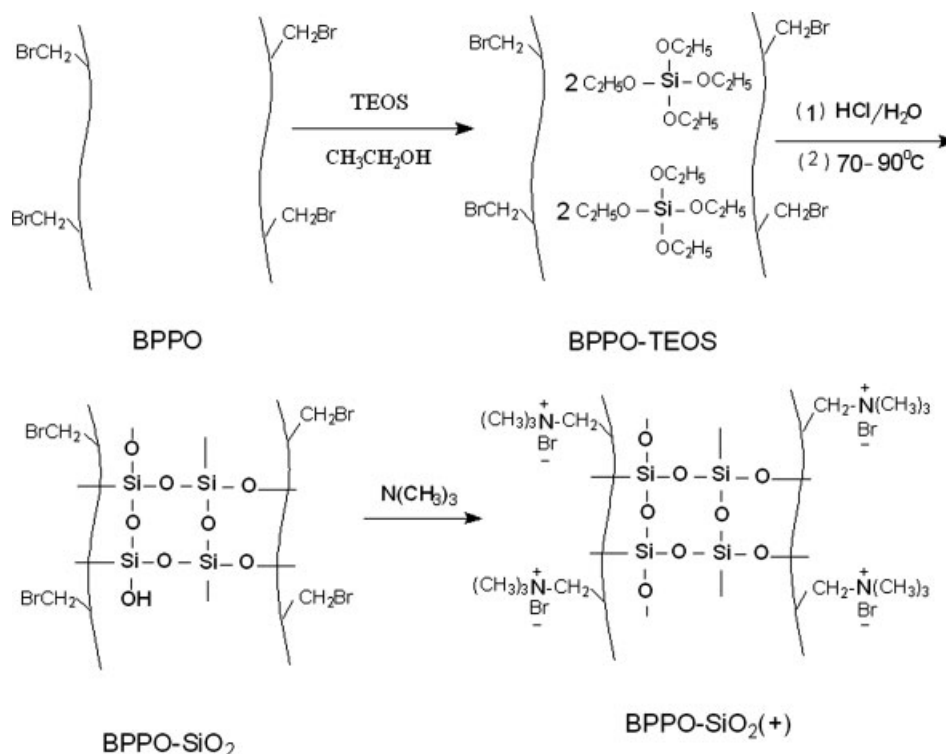


Figure 2 Preparation procedures for hollow-fiber anion-exchange hybrid membranes from BPPO.

flow and at a heating rate of 10°C/min. The morphologies of the base hollow fibers and some further aminated ones were observed with scanning electron microscopy (XT30 ESEM-TMP, Philip, Amsterdam, The Netherlands). Samples were cut into small pieces and coated with gold before cross-section observation. If not specifically mentioned, the hybrid hollow-fiber samples for characterizations were obtained by the treatment of the hollow-fiber base membranes with a 25% TEOS–C<sub>2</sub>H<sub>5</sub>OH solution at room temperature for 12 h, including the samples before the sol–gel process, after the sol–gel process, and after further amination.

### IEC

IEC was determined by the Mohr method.<sup>18</sup> The final hollow-fiber hybrid membranes in the chloride form were converted to the sulfate after immersion in a 0.5 mol/L Na<sub>2</sub>SO<sub>4</sub> solution. The chloride ions released from the fibers were determined by titration with a 0.1M AgNO<sub>3</sub> solution with K<sub>2</sub>CrO<sub>4</sub> as an indicator. IECs were calculated from the released chloride ions with the following equation:

$$\text{IEC} = \frac{V_{\text{Ag}} C_{\text{Ag}}}{W_4} \text{ (mmol/g of dry weight in the Cl}^- \text{ form)} \quad (1)$$

where  $V_{\text{Ag}}$  and  $C_{\text{Ag}}$  are the volume and concentration of the AgNO<sub>3</sub> solution, respectively, and  $W_4$  is the dry weight of the final fiber [BPPO–SiO<sub>2</sub>(+)] in the Cl<sup>−</sup> form.

### Weight gain and water content

There are four kinds of weights denoted in this article:  $W_1$  is the dry weight of the base BPPO,  $W_2$  is the dry weight of BPPO–SiO<sub>2</sub> (after the sol–gel process), and  $W_3$  and  $W_4$  are the wet and dry weights of the final aminated sample [BPPO–SiO<sub>2</sub>(+)]. To describe the weight changes after the sol–gel and amination processes, two weight gains were defined. The first weight gain ( $W_{g1}$ ) indicates an increase in the hollow-fiber weight due to the incorporation of TEOS. It was calculated from the dry weight difference between the base fiber ( $W_1$ ) and the fiber after the sol–gel process ( $W_2$ ):

$$W_{g1} = \frac{W_2 - W_1}{W_1} \quad (2)$$

where the second weight gain ( $W_{g2}$ ) indicates a weight change due to amination and was calculated from the dry weight difference between the final aminated fiber ( $W_4$ ) and the fiber after the sol–gel process ( $W_2$ ):

$$W_{g2} = \frac{W_4 - W_2}{W_2} \quad (3)$$

The water content was determined from the weight difference between the wet weight ( $W_3$ ) and the dry weight ( $W_4$ ) of the aminated fiber [BPPO–SiO<sub>2</sub>(+)] in units of grams of H<sub>2</sub>O/grams of dry fibers (in the Cl<sup>−</sup> form). The equation used for calculation is as follows:

$$\text{WR} = \frac{W_3 - W_4}{W_4} \quad (4)$$

### Dimensional stability

There are also four kinds of lengths denoted in this article:  $L_1$  is the length of the dry base BPPO,  $L_2$  is the length of the dry BPPO–SiO<sub>2</sub> (after the sol–gel process), and  $L_3$  and  $L_4$  are the lengths of the final wet and dry samples [BPPO–SiO<sub>2</sub>(+)]. Our experimental results show that the dimensional change during the sol–gel process was negligible [such a dimensional change ratio (DCR) was within 0.3–0.7%]. Therefore, in this study, DCR was calculated from  $L_3$  and  $L_1$ :

$$\text{DCR} = \frac{L_3 - L_1}{L_1} \times 100\% \quad (5)$$

## RESULTS AND DISCUSSION

As described in the Experimental section, we prepared the final fibers by soaking the base fiber with TEOS solution and then aminating the fiber. Because it was possible for some adsorbed TEOS to leach out through the fiber in the subsequent processes, it was difficult to precisely determine the fiber's silica content. Also, it would be inconvenient for others to repeat the experiment if silica content was used instead of TEOS concentration. Our preliminary test also showed that the weight gain after the sol–gel reactions increased with increasing TEOS concentration, so in the following sections, discussions are made on the basis of TEOS concentration instead of the exact silica content.

### FTIR

To confirm the step reactions, the base fibers and the products in each step were characterized by FTIR, and the spectra for the base hollow fibers and the hybrid fibers are shown in Figure 3. Before FTIR analysis, all of the samples were conditioned in a 25% TEOS–C<sub>2</sub>H<sub>5</sub>OH solution at room temperature for 12 h. In all of the spectra, the characteristic vibrations of the BPPO units were observed at about

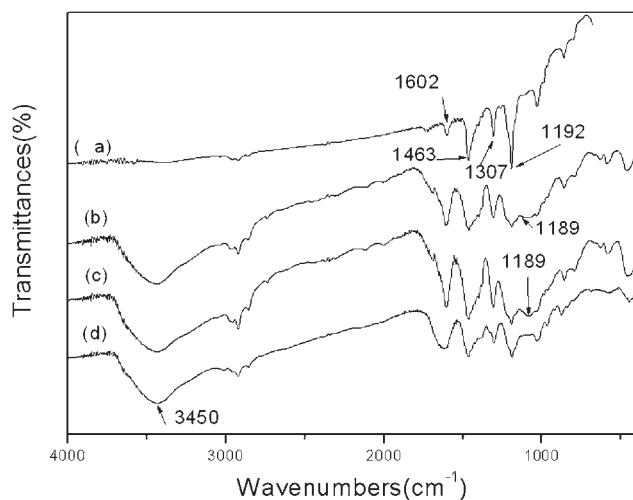


**Figure 3** FTIR spectra of (a) BPPO (the base fiber), (b) BPPO-TEOS (the fiber was immersed in a 25% TEOS- $C_2H_5OH$  solution at room temperature for 12 h before the sol-gel process), (c) BPPO- $SiO_2$  (the fiber was immersed after the sol-gel process), and (d) BPPO- $SiO_2(+)$  (the final hybrid membrane after amination).

1602, 1463, 1307, and 1192  $cm^{-1}$ .<sup>19</sup> As compared to the curve in Figure 3(a), some strong absorption bands appeared in the range 1150–950  $cm^{-1}$  shown in Figure 3(b); moreover, the peak at about 1189  $cm^{-1}$  became broader. These bands and peaks were characteristic of TEOS: 1165  $cm^{-1}$  ( $Si-O-C$  rocking), 1105  $cm^{-1}$  [ $\nu_a(C-C-O)$ ,  $\delta(COH)$ ], 1082  $cm^{-1}$  [ $\nu_a(SiO-CO)$ ], and 968  $cm^{-1}$  [ $\delta(H_3CO)$ ,  $\delta(H_3CC)$ ].<sup>20–22</sup> As for the strong band at about 3450  $cm^{-1}$  shown in Figure 3(b), it was ascribed to  $-Si-OH$  or  $-OH$  groups from the remaining ethanol. When BPPO was immersed in TEOS, trace water in the air may have been introduced into the reaction system, and then, the unstable alkoxy silane [ $Si(OCH_2CH_3)_3$ ] groups were likely to hydrolyze or even condense partly and form  $-Si-OH$  groups.

When Figure 3(c) is compared with Figure 3(b), no new absorption peak can be recognized because the characteristic peaks associated with  $Si-O-Si$  or  $Si-OH$  groups, such as  $\nu_a(Si-O-Si)$  ( $\sim 1066$   $cm^{-1}$ ) and  $\nu(Si-OH)$  (940–960  $cm^{-1}$ ), were also in the range 1150–950  $cm^{-1}$ . Nonetheless, the peak at about 790  $cm^{-1}$  [ $\nu_s(Si-O-Si)$ ] increased to some extent;<sup>22,23</sup> the peak at about 1189  $cm^{-1}$ , which was broader in Figure 3(b), shrank slightly in Figure 3(c). This was because the absorption of  $Si(OCH_2CH_3)_3$  groups (1165  $cm^{-1}$ ,  $Si-O-C$  rocking) disappeared.

After quaternary amination, the peak of hydroxyl groups at about 3450  $cm^{-1}$  strengthened significantly [Fig. 3(d)], but the bands in the range 1150–950  $cm^{-1}$  became weaker than those in Figure 3(c). This was mainly because some silica components leached out during the reaction with an aqueous solution of

$N(CH_3)_3$ . The peak of  $\nu(-N^+-CH_3)$  at 1440  $cm^{-1}$  overlapped the peak from the polymer chain ( $-1466$   $cm^{-1}$ ) and thus could not be clearly recognized. The IEC values of hybrid membranes confirmed the reaction of quaternary amination.

### Thermogravimetric analysis (TGA)

The thermal stability of the hollow-fiber hybrid membranes (treated with a 25% TEOS- $C_2H_5OH$  solution before the sol-gel process) before and after amination was measured with TGA under an air atmosphere, and the results are shown in Figure 4(b,d). For comparison, the TGA results of the base BPPO fiber and its aminated one are also presented in Figure 4(a,c). The thermal degradation temperature ( $T_d$ ) of BPPO was about 240°C under an air atmosphere, and that of the prepared hybrid hollow fibers after TEOS treatment and the sol-gel process (BPPO- $SiO_2$ ) was about 251°C. This increase in  $T_d$  was due to formation of a  $Si-O-Si$  network in the matrix. After quaternary amination, the thermal stability of the final hollow-fiber anion-exchange hybrid membrane decreased to some extent ( $T_d = 198^\circ C$ ). Such a decrease in  $T_d$  may have been due to the existence of quaternary amine groups, which were relatively thermally unstable. As compared to quaternized BPPO, which had a  $T_d$  around 193°C, the final hollow-fiber anion-exchange hybrid membrane had a higher  $T_d$ . Therefore, the hybrid membrane showed better thermal stability than the corresponding polymeric membrane; that is, the formation of the silica network by the incorporation of TEOS in

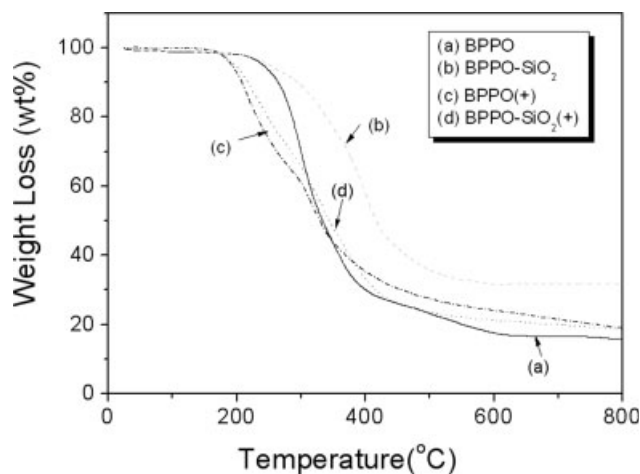


**Figure 4** TGA thermograms of (a) BPPO (the base fiber), (b) BPPO- $SiO_2$  (the BPPO base fiber after immersion in a 25% TEOS- $C_2H_5OH$  solution at room temperature for 12 h and then the sol-gel process), (c) BPPO after quaternary amination, and (d) BPPO- $SiO_2(+)$  (final hybrid membrane of BPPO- $SiO_2$  after amination).

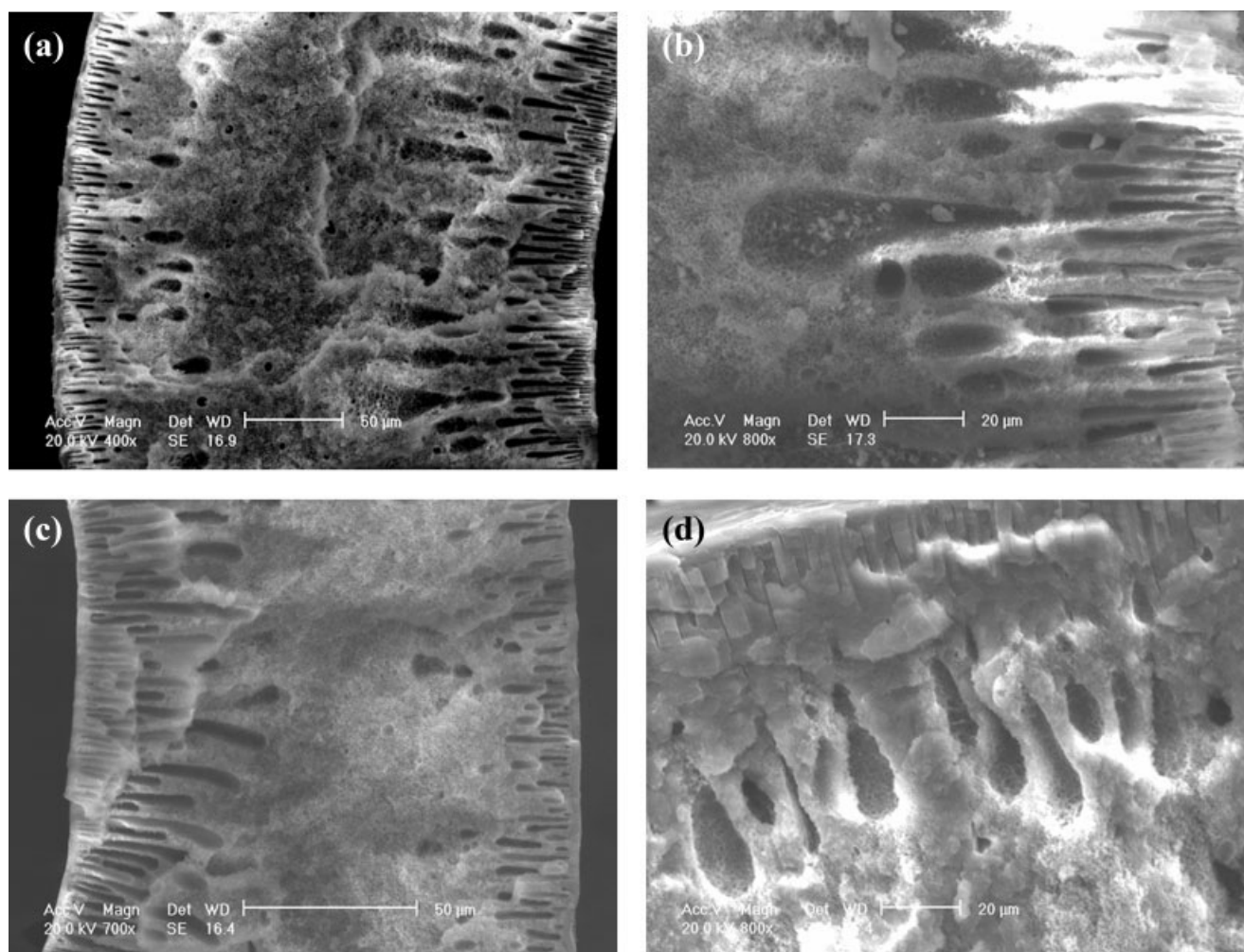


**Figure 5** SEM images of hollow fibers: (a) BPPO (the base fiber), (b) BPPO-TEOS (the fiber was immersed in a 25% TEOS- $C_2H_5OH$  solution at room temperature for 12 h before the sol-gel process), (c) BPPO- $SiO_2$  (the fiber was immersed after the sol-gel process), and (d) BPPO- $SiO_2(+)$  (the final hybrid membrane after amination).

the BPPO base hollow fibers enhanced the thermal stability.

### SEM

For the hollow-fiber hybrid membranes, not only is sufficient adhesion between the organic-inorganic hybrid layer essential for physical stability but also enough compatibility between the organic and inorganic phases is necessary for membrane chemical stability. Particularly, practical applications with diffusion dialysis require the hollow-fiber membranes to have a homogeneous and denser structure than the conventional hollow-fiber membranes designed for ultrafiltration or microfiltration. To obtain the microstructure, SEM was used to observe the cross section of the hollow fibers. Our preliminary tests indicated that there were many similarities in SEM images between the hollow-fiber hybrid membranes treated with TEOS and the corresponding aminated samples, so only the image was randomly selected

as an example (TEOS, 25 v/v %). Figure 5 shows the cross section of a base hollow fiber (BPPO) and those of BPPO-TEOS, BPPO- $SiO_2$ , and BPPO- $SiO_2(+)$ . Generally speaking, during phase inversion, the base hollow fibers contained many visible pores and cavities; naturally, fine pores may have existed. In our previous studies,<sup>17</sup> the hollow fibers before amination possessed relatively high water contents (ca. 49.6%) due to capillary tension. This may have been the reason why the image of the base hollow fiber was a little darker in color [Fig. 5(a)]. After immersion in a TEOS solution, the fiber's water content seemed to decrease because of the incorporation of TEOS. Some of the TEOS was not dispersed homogeneously and existed as particles [Fig. 5(b)]. However, after hydrolysis and condensation with water/HCl as the catalyst, the hybrid hollow-fiber BPPO- $SiO_2$  appeared homogeneous and had no recognizable silica particles [Fig. 5(c)]. The pores were filled with silica partially because a Si-O-Si network formed in the membrane matrix, and thus, the

pore fraction seemed to diminish. After further amination with TMA, the formed trimethylbenzylammonium groups were more hydrophilic and made the organic phase swellable, but the inorganic Si—O—Si network contributed to the dimensional stability of the fiber. So the final result is that the initial pores in the base hollow fibers disappeared because of the swelling of the organic phase and the final hollow-fiber membranes became denser, as shown in Figure 5(d).

For the investigated hybrid system, the formed Si—O—Si network was more hydrophobic compared to the aminated BPPO. This caused a problem in the compatibility between inorganic and polymer phases. However, in the sol-gel process, more Si—OH groups were formed simultaneously, and these groups added to the hydrophilicity. Furthermore, as described later, not all of the bromomethylated groups in BPPO were involved in amination. A relatively high portion of bromomethylated groups remained unchanged and contributed to the hydrophobicity. Hence, as presented in Figure 5(d), the final hollow-fiber membranes showed good compatibility.

### Weight gain

To prove the existence of inorganic silica in the base organic hollow fibers, the weight changes after the sol-gel process were determined, and the results are illustrated in Figure 6(a). With an increase in TEOS concentration, the weight gain increased. In the experiment, the maximum weight gain attained was as high as 17% when the TEOS concentration was equal to 45% v/v. This suggested that the higher the TEOS concentration was, the greater the amount of TEOS that entered the matrix was. After the sol-gel process, more inorganic silica phases were formed in the organic matrix, and this increased the total weight of the fiber. Surprisingly, the base hollow fiber, which followed the same treatment procedure but with a TEOS concentration of 0, had a negative value. This may have been caused by the weight decrease of the base fiber after treatment; that is, some impurities, such as small-molecule (brominated) poly(2,6-dimethyl-1,4-phenylene oxide) in the base hollow fiber, were removed. Correspondingly, the practical weight gain due to TEOS incorporation was a little higher than the experimental values. Such impurities only accounted for 0.69% (the weight gain for the base fiber was around  $-0.69\%$ ). Such a value was too small to change any trend in the experiment.

After amination, all of the samples had positive weight gains; however, the changing trend was opposite to that discussed previously [Fig. 6(b)]: the higher the TEOS concentration was, the lower the increase in weight was. There were two reasons for this. First, although the total number of bromome-

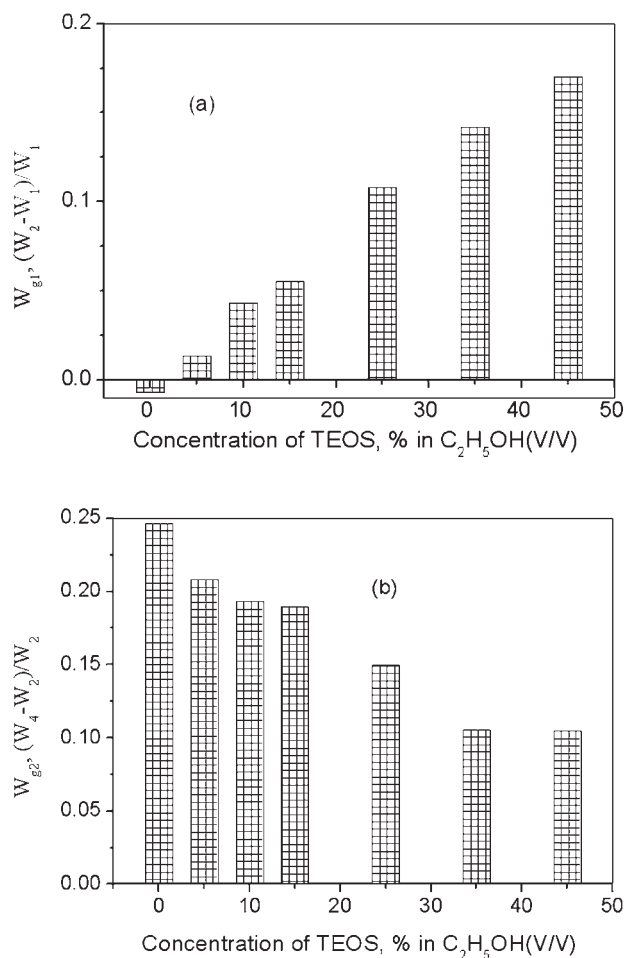


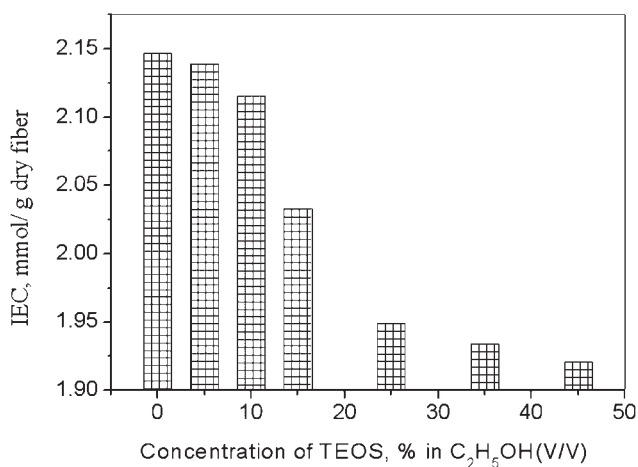
**Figure 6** Weight gains of hollow fibers treated with different concentrations of TEOS: (a) after the sol-gel process and (b) after amination.

thylated groups in the base fiber had not reacted with TMA, the incorporation of TEOS in the matrix still made the fiber more compact. The water content decreased as the TEOS concentration increased, and more Si—O—Si networks were formed. These networks were steric hindrance for the quaternary reaction, as verified by the IEC values hereafter. Second, there was a change in the composition of the hollow fibers. As shown previously, the higher TEOS concentration was, the higher the weight gain after the sol-gel process was (i.e., a higher increase in silica content). This led to a decrease in the BPPO content; hence, after amination, a fiber having a higher silica content had a lower weight gain. These trends conformed to eq. (3), in which the weight gain after amination decreased as  $W_2$  increased.

The change in weight gain was confirmed by the change in IEC and water content, as discussed later.

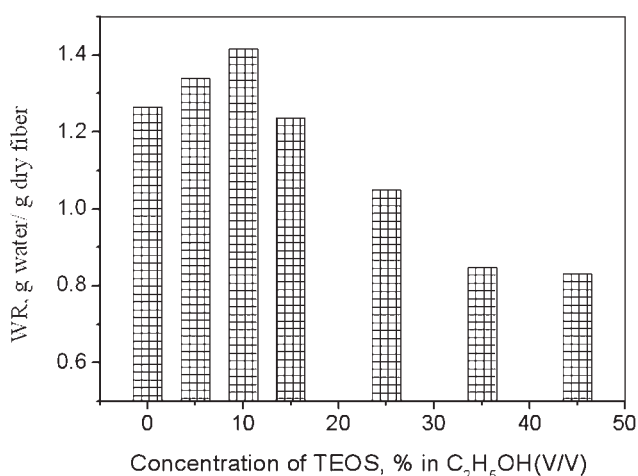
### IEC and water content

Figure 7 illustrates the IECs of the final hollow-fiber hybrid membranes. With an increase in TEOS



**Figure 7** IEC of BPPO-SiO<sub>2</sub>(+) treated with different concentrations of TEOS.

concentration, IEC decreased. The trend was the same as that for the weight gain due to amination ( $W_{g2}$ ) and could be explained in the same way: an increase in the content of the BPPO-SiO<sub>2</sub> hybrid resulted in a decrease in the portion of the organic phase, and the network formed made the fiber more compact. Those two reasons were responsible for the IEC decrease with an increase in TEOS concentration. Nonetheless, the magnitude of change was not so significant. For the samples in this investigation, the values of IEC changed from 2.15 mmol/g of dry fiber (base BPPO fibers) to 1.92 mmol/g of dry fiber (the fiber treated with 45 v/v % TEOS). The material used in this experiment was a mixture of D9010 (90% benzyl substitution and 10% aryl substitution) and 9020 (90% benzyl substitution and 20% aryl substitution) with a weight ratio of 0.42 : 0.38. The theoretical IEC value was estimated to be 3.1–3.5 mmol/g with full amination. Obviously, the yield of amination was lower than 100%. However, this will not



**Figure 8** Water content (WR) of BPPO-SiO<sub>2</sub>(+) treated with different concentrations of TEOS.

prevent such hollow-fiber membranes from application because the famous anion-exchange membrane AMX from Tokuyama (Japan) only has an IEC of about 1.6 mmol/g of dry weight.

The water contents of the final hollow-fiber anion-exchange hybrid membranes are illustrated in Figure 8. Initially, the water content increased as the TEOS concentration increased, but it decreased when the TEOS concentration was higher than 10%. Such a changing trend was different from that for IEC. It was not difficult to understand the decrease at high TEOS concentrations because the IEC was proportional to water content and decreased at this stage. When the TEOS concentration was less than 10%, IEC decreased slightly (from 2.14 to 2.11, as shown in Fig. 7), but the increase in the weight gain after the sol-gel process seemed a little higher [0.7–4.3%, as shown in Fig. 6(a)]. Although such a weight gain was still not enough to form well-organized Si—O—Si networks and many of them existed in the form of hydroxyl silica (—Si—OH), this hydroxyl silica was hydrophilic and responsible for a slight increase in the water content at low TEOS concentrations. To summarize, the water contents were determined by two factors: (1) at low TEOS concentrations, an increase in the amount of —Si—OH groups resulted in an increase in the water content, and (2) at high TEOS concentrations, a decrease in the amount of trimethylbenzylammonium groups (due to the weight gain after the sol-gel process) gave rise to a decrease in the water content.

## DCR

For practical applications, it is required that hollow-fiber membranes have dimensional stability. As shown in Figure 9, DCR decreased as the TEOS concentration increased. The explanation was the same

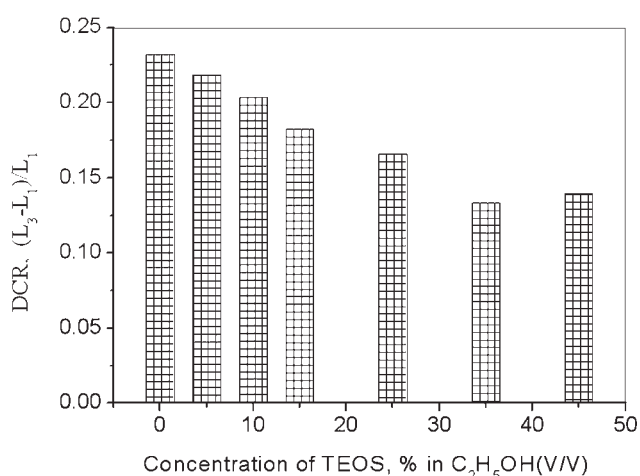


**Figure 9** DCR of BPPO-SiO<sub>2</sub>(+) treated with different concentrations of TEOS.



as discussed previously: an increase in the TEOS concentration was favorable for the formation of Si—O—Si networks and made the final hollow-fiber membranes more dimensionally stable. If the TEOS concentration was controlled in the range 25–45 wt %, the final hollow-fiber hybrid membranes had a DCR ranging from 13 to 16%.

In our previous study,<sup>17</sup> polymeric hollow-fiber membranes were prepared from similar base fibers. In that case, to retain the dimensional stability, the hollow fibers were aminated with dimethylethanolamine, and some were further aminated with TMA. Under optimum conditions, the membranes had the following properties: IEC = 2.2–2.5 mmol/g, water content = 0.6–0.8 g of water/g of dry weight, and DCR = 18–20%. Obviously, in this research, the hollow-fiber hybrid membranes had a relatively higher dimensional stability, although they possessed relatively higher water contents. In this sense, this research provides another method for controlling the dimensional stability of hollow-fiber membranes. The construction of hollow-fiber modules and the investigation of their separation performance are underway.

### CONCLUSIONS

A novel route for preparation of hollow-fiber anion-exchange hybrid membranes was examined, and the procedure included the immersion of BPPO base hollow fibers in a TEOS–ethanol solution and subsequent sol–gel and quaternary amination. The prepared hollow-fiber anion-exchange hybrid membranes had (1) good compatibility between the inorganic silica and organic phase by the formation of Si—O—Si networks within fiber matrix and (2) relatively high thermal and dimensional stabilities. The main properties, including IEC and water content, were related to TEOS concentration. The recommended TEOS concentration is in the range 15–45% in ethanol, and the membrane obtained had IECs of 1.9–2.0 mmol/g of dry weight, water contents of

0.83–1.23 g of water/g of dry weight, and DCRs of 13–16%. Further studies will focus on the application of such hybrid hollow-fiber membranes under severe conditions, such as the recovery of acid from industrial waste at high temperatures by diffusion dialysis.

The authors give special thanks to Cuiming Wu for analyzing the FTIR data and Chuanhui Huang for proofreading the manuscript.

### References

1. Helfferich, F. *Ion-Exchange*; McGraw-Hill: London, 1962.
2. Strathmann, H. *Ion-Exchange Membrane Separation Processes*; Membrane Science and Technology Series 9; Elsevier: Amsterdam, 2004.
3. Huang, C. H.; Xu, T. W.; Zhang, Y. P.; Xue, Y. H.; Chen, G. W. *J Membr Sci* 2007, 288, 1.
4. Saracco, G. *Ann Chim Rome* 2003, 93, 817.
5. Xu, T. W. *J Membr Sci* 2005, 263, 1.
6. Xu, T. W. In *Trends in Conservation and Recycling of Resources*; Loeffe, C. V., Ed.; Nova Science: New York, 2006; p 99.
7. Wen, J.; Wilkes, G. L. *Chem Mater* 1996, 8, 1667.
8. Ohya, H.; Paterson, R.; Nomura, T.; McFadzean, S.; Suzuki, T.; Kogure, M. *J Membr Sci* 1995, 105, 103.
9. Kogure, M.; Ohya, H.; Paterson, R.; Hosaka, M.; Kim, J.; McFadzean, S. *J Membr Sci* 1997, 126, 161.
10. Kickelbick, G. *Prog Polym Sci* 2003, 28, 83.
11. Honma, I.; Hirakawa, S.; Yamada, K.; Bae, J. M. *Solid State Ionics* 1999, 118, 29.
12. Wu, C. M.; Xu, T. W.; Liu, J. S. In *Focus on Solid State Chemistry*; Newman, A. M., Ed.; Nova Science: New York, 2006; p 1.
13. Wu, C. M.; Xu, T. W.; Gong, M.; Yang, W. H. *J Membr Sci* 2005, 247, 111.
14. Wu, C. M.; Xu, T. W.; Yang, W. H. *J Membr Sci* 2003, 216, 269.
15. Wu, C. M.; Xu, T. W.; Yang, W. H. *J Membr Sci* 2003, 216, 269.
16. Lhang, Z. S.; Xu, T. W.; Wu, C. M. *J Membr Sci* 2006, 269, 142.
17. Xu, T. W.; Liu, Z. M.; Huang, C. H.; Wu, Y. H.; Wu, L.; Yang, W. H. *Ind Eng Chem Res* 2008, 47, 6204.
18. Doughty, H. W. *J Am Chem Soc* 1924, 46, 2707.
19. Xu, T. W.; Zha, F. F. *J Membr Sci* 2002, 199, 203.
20. Rubio, F.; Rubio, J.; Oteo, J. L. *Spectrosc Lett* 1998, 31, 199.
21. Chu, P. Y.; Clark, D. E. *Spectrosc Lett* 1992, 25, 201.
22. Innocenzi, P. *J Non-Cryst Solids* 2003, 316, 309.
23. Matos, M. C.; Ilharco, L. M.; Almeida, R. M. *J Non-Cryst Solids* 1992, 147, 232.